Numerical Methods in Civil Engineering

Projected changes in precipitation and air temperature over the Volga River Basin from bias-corrected CMIP6 outputs

S. Mahya Hoseini[*], Mohsen Soltanpour[**], Mohammad R. Zolfaghari[***]

ARTICLE INFO

RESEARCH PAPER

Article history:
Received:
October 2023
Revised:
November 2023
Accepted:
January 2024

Keywords:
Climate change,
CMIP6,
Precipitation,
Temperature,
Uncertainty,
Volga River basin,
Precipitation,
Temperature

Abstract:

This paper investigates future changes in annual mean precipitation and air temperature across the Volga River basin, which serve as significant drivers of climate-induced changes in the Volga River's discharge, the primary input to the Caspian Sea. The thirteen Global Climate Models (GCMs) outputs under four Shared Socioeconomic Pathways (SSPs) scenarios (SSP1–2.6, SSP2–4.5, SSP3–7.0, and SSP5–8.5) from the sixth phase of Coupled Model Intercomparison Project (CMIP6) were used for this study. In the historical period (1950-2014), using comprehensive rating metrics and Taylor diagram, the GCMs are ranked according to their ability to capture the temporal and spatial variability of precipitation and air temperature. The Multi-Model Ensemble (MME) is generated, and bias-correction techniques are utilized to reduce the uncertainties and correct the biases in CMIP6 outputs. Bias-correction techniques were assessed during the historical period and an average of appropriate methods were utilized for future projections (2015-2100). In the 21st century, future projections show that the Volga River basin could mainly experience a temperature increase of 0.4°C to 7.5°C, alongside a precipitation rise of 0.7% to 37%, depending on the scenarios considered. A comparison of future projections with an observational dataset from 2015 to 2017 indicates that the SSP2–4.5 is a more likely scenario to represent the future climate of the Volga River basin.

1. Introduction

Recently, the study of climate change's impact on temperature and precipitation and its consequences for the human environment has gained prominence as a vital research area (1–3). Changes in main climate parameters like precipitation, temperature, and evapotranspiration significantly affect the basin's runoff (4). Accurately predicting future precipitation and air temperature changes is vital for managing climate-related risks through adaptation and mitigation strategies. General Circulation Models (GCMs) are essential for understanding and studying the consequences of past, current, and future climate change (5).

* *Corresponding Author: PhD candidate in Coastal Engineering, Civil Engineering Department, K. N. Toosi University of Technology, Tehran, IRAN, Email: sm.hoseini@mail.kntu.ac.ir*

** *Professor, Civil Engineering Department, K. N. Toosi University of Technology, Tehran, IRAN*

*** *Associate Professor, Civil Engineering Department, K. N. Toosi University of Technology, Tehran, IRAN*

Despite several improvements that have been made in the latest sixth phase of the Coupled Model Intercomparison Project (CMIP6), significant uncertainties and biases still exist in GCMs' historical and future simulations (6). Uncertainties and biases in GCMs stem from their low resolutions, parameterization schemes, boundary conditions, carbon cycles representations, and the insufficient theoretical understanding of the Earth's climate (7). Some techniques including bias correction, appropriate GCM selection, and the generation of multi-model ensembles (MME) have been employed to reduce these biases and uncertainties (Mishra *et al.*, 2020; Raju and Kumar, 2020). Recently, MMEs of GCMs have become the preferred approach over single GCMs for improving future projections (10).

The Volga region is a vital area for Russia's population and economy, warming 2.5 times faster than the global average, as assessed by Roshydromet (11). Climate variations in this region impact living conditions and activities, notably affecting water flow. The Volga's flow accounts for 80% of the Caspian Sea's water inflow (12). Changes in the climate

https:doi.org/10.52547/NMCE.2303.1034

within its basin and its discharge cause significant fluctuations in the Caspian Sea level.

Studies on the future changes in the Volga River basin's precipitation and temperature are limited. Nesterenko *et al.* (2023) analyzed annual air temperature and precipitation changes over the Volga and Urals basins, using observational data from 1887 to 2020. They found that over this period, the average annual air temperature has increased 1.8°C, with winter temperatures rising 2.3°C and summer temperatures rising 1°C. Additionally, during this period, annual precipitation in forest and steppe zones increased by an average of 55 mm, primarily due to heightened winter precipitation. Analyzing river gauge data, Georgiadi *et al.* (2019) discovered that during the current climate warming period (since 1981), there was a 3.4% increase in annual runoff compared to the reference period (1930-1980). Changes in the Volga River runoff was also assessed using CMIP5-GCMs under RCP2.6[1] and RCP8.5 future scenarios. The analysis indicates that from 2010 to 2039, the Volga River annual runoff may slightly increase compared to the 1960-1990 period, with an estimated rise of 2-10% depending on the scenario (15). Kalugin (2022) used the precipitation and temperature outputs of two CMIP5-GCMs, including GFDL-ESM2M and MIROC5, over the Volga River basin to assess climate change impacts on the Volga River runoff in the 21st century. Kalugin (2022) reported that in the projected global warming scenarios of 1.5°C and 2°C by 2045 and 2064, the Volga basin could experience mean annual air temperature increases of 2.5 °C and 3.4 °C, respectively. Annual precipitation in the Volga basin increases by 8% at 1.5 °C global warming and averages 11% at 2 °C global warming. Although precipitation has increased, their simulated annual Volga runoff has reduced by 10-11% in both scenarios compared to the levels from 1970-1999. This result suggests that evaporation will play a more significant role in the Volga basin's water balance.

The limitations of previous studies include the limited utilization of GCMs and climate change scenarios, the lack of evaluation models and the construction of multi-model ensembles, and the absence of GCM bias correction. To address the limitations of previous studies, this study aims to investigate the projected changes in precipitation and air temperature in the Volga River basin using CMIP6-GCMs under different climate change scenarios. First the ability of CMIP6-GCMs to simulate spatial and temporal variabilities in temperature and precipitation is evaluated during the historical period (1950-2014). Then, a subset of appropriate GCMs is utilized to produce a multi-model ensemble for precipitation and temperature. The multi-model ensemble is corrected for bias using efficient techniques based on spatial and temporal evaluation. Future changes in air temperature and precipitation are investigated by analyzing the corrected multi-model ensemble in the near (2020-2046), mid (2047-2073), and far (2074-2100) periods relative to the reference period (1988-2014).

This paper is organized as follows: Section 2 presents the study area and data, Section 3 outlines the methodology, and Section 4 summarizes the results and discussions.

2. Study Area and Data

2.1 Volga River Basin

The Volga River is Europe's largest river by basin area (1,360,000 km^2), length (3530 km), and annual water volume (250 km^3). It is situated within the geographic coordinates of 48◦ to 62◦ N and 32◦ to 60◦ E (Fig. ***1*** (a)). The river's source is located at an elevation of 228 m above sea level, while its mouth, where it flows into the Caspian Sea, is 28 m below sea level (16).

The Volga River provides 80% of the water budget input to the Caspian Sea (12). Precipitation and temperature variations within the Volga River basin substantially impact its discharge, leading to the Caspian Sea level fluctuations. The Volga River basin encompasses some climate regions according to the Köppen Climate Classification (17). Its primary climate is continental, with a small area in the basin's southern part having an arid climate (Fig. ***1***(a)). The Volga basin has an average annual air temperature of 3.4°C and receives an annual precipitation of 567 mm, calculated from the GHCN[2] observational dataset from 1950 to 2014. Fig. ***1*** (b,c) displays the spatial distribution of annual mean air temperature and precipitation.

2.2 Climate models and observational dataset

The data from GCMs, covering historical simulations (1850 to 2014) and future scenarios (2015 to 2100), is sourced from the latest phase of the Coupled Model Intercomparison Project, CMIP6 (18). CMIP6's future projections include Shared Socioeconomic Pathways (SSPs) as well as specific targets for radiative forcing by the end of the 21st century (O'Neill *et al.*, 2016). The study employs a range of scenarios, namely SSP1-2.6, SSP2-4.5, SSP3-7.0, and SSP5-8.5. Each scenario represents distinct combinations of radiative forcing and development pathways. SSP1-2.6 portrays a future characterized by low levels of forcing and a commitment to sustainable development. SSP2-4.5 reflects a moderate forcing scenario with a middle-of-the-road development trajectory. SSP3-7.0 represents a scenario with medium-to-high-end levels of forcing, accompanied by regional rivalry. Lastly, SSP5-8.5 illustrates a high-end forcing scenario driven by fossil fuel-dependent

[1] Representative Concentration Pathway

[2] Global Historical Climate Network

development. Descriptions of the models used in this study are presented in Table 1. Model selection depends on data availability for scenarios and the historical period in the Volga River basin. CMIP6 data is obtained from the Earth System Grid Federation (ESGF) website at https://esgf-node.llnl.gov/search/cmip6 (last access date: 2023/10/1). Many GCMs comprise various ensembles based on different realizations, initialization methods, and model physics. The mean of all available ensembles is calculated for each climate model.

To assess GCM simulations, gridded datasets with suitable homogenization and interpolation are typically preferred due to the limitations arising from the spatial non-uniformity in station observations (20). In this study, historical simulations of CMIP6-GCMs are assessed using the Global Historical Climate Network (GHCN) dataset (21) at a spatial resolution of 0.5°×0.5°. The prior studies have demonstrated the performance of air temperature and precipitation of the GHCN datasets in evaluating CMIP6-GCMs (e.g., Muche et al., 2020; S. Wang et al., 2022; Liang-Liang et al., 2022). The GHCN dataset can be accessed at https://psl.noaa.gov/data/gridded/data.UDel_AirT_Precip.html#detail (last access date: 2023/10/1).

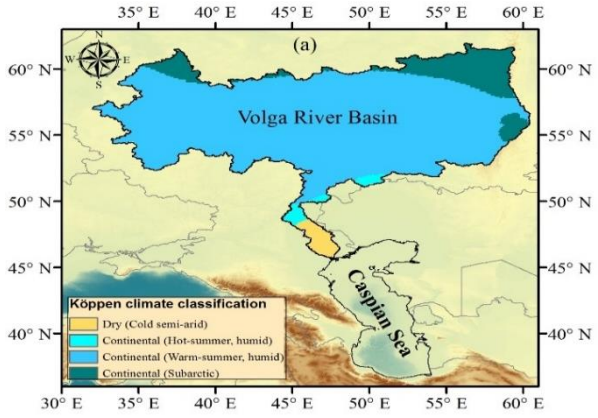

(a)

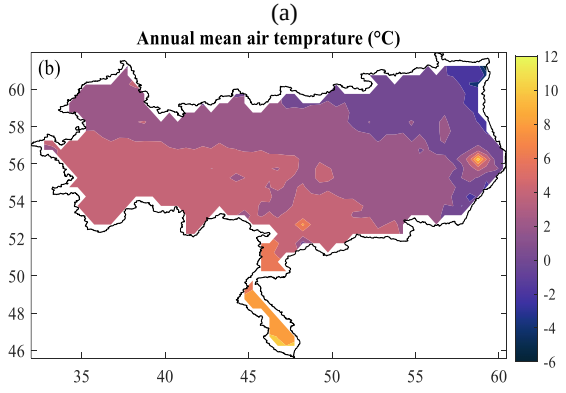

(b)

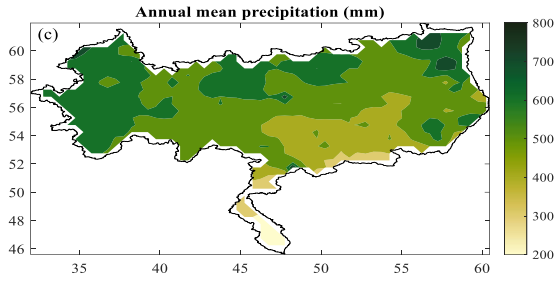

(c)

Fig. 1: (a) The location of the Volga River basin and its climate classes based on the Köppen Climate Classification, (b) observed annual mean air temperature (°C), and (c) precipitation (mm) during 1950-2014

3. *Methodology*

This study developed a bias-corrected dataset of precipitation and air temperature over the Volga River basin, using output from 13 CMIP6-GCMs under four scenarios (SSP1–2.6, SSP2–4.5, SSP3–7.0, and SSP5–8.5) for both the historical (1950–2014) and future periods (2015–2100). The study involves ranking the GCMs based on performance and implementing bias correction techniques. To address significant sources of uncertainty, including the choice of climate models and bias correction methods, all available CMIP6 models and a variety of bias correction techniques are utilized. This ranking process leads to the forming a multi-model ensemble comprising the most reliable models. Bias correction techniques are then applied to reduce biases. The initial step involves interpolating the GCM outputs to a 0.5 * 0.5 grid resolution to align with the spatial resolution of GHCN observational dataset grids. Subsequently, historical CMIP6 model outputs for precipitation and temperature are assessed against observational reference data, in terms of temporal and spatial assessments. Temporal evaluation is performed by the comprehensive rating metrics (25), which ranks models based on criteria such as Correlation Coefficients (CC), Mean Absolute Errors (MAE), bias, Root Mean Square Errors (RMSE), and Standard Deviations (SD). Spatial assessment employs Taylor diagrams (26) to assess CC, SD, and centered Root Mean Square Difference (RMSD). In the final step, models that effectively reproduce both temporal and spatial patterns are selected for generating the multi-model ensemble (MME). The study additionally applies and evaluates bias correction methods, adopting the mean of the outputs from the most effective techniques, referred to as "mean_methods," for utilization in future projections. The corrected temperature and precipitation projections are examined to investigate the influence of climate change on the Volga River basin, which is valuable for future assessments of Volga River discharge in light of climate change. Details of the suggested approaches are explained in the following sections.

Table 1: Description of CMIP6 models used in this study

Model	Key References	Horizontal Resolution (lat. × lon.)
BCC-CSM2-MR	(27)	$1.125^{\circ} \times 1.125^{\circ}$
CanESM5	(28)	$2.8^{\circ} \times 2.8^{\circ}$
CESM2	(29)	$1.4^{\circ} \times 1.4^{\circ}$
CNRM-CM6-1	(30)	$1.4^{\circ} \times 1.4^{\circ}$
CNRM-ESM2-1	(31)	$1.4^{\circ} \times 1.4^{\circ}$
FGOALS–g3	(32)	$2.8^{\circ} \times 2.8^{\circ}$
GISS-E2-1-G	(33)	$1.125^{\circ} \times 1.125^{\circ}$
HadGEM3–GC31–LL	(34)	$1.875^{\circ} \times 2.5^{\circ}$
IPSL–CM6A–LR	(35)	$1.26^{\circ} \times 2.5^{\circ}$
MIROC6	(36)	$1.25^{\circ} \times 1.875^{\circ}$
MIROC-ES2L	(37)	$2.25^{\circ} \times 2^{\circ}$
MRI-ESM2-0	(38)	$1.25^{\circ} \times 0.94^{\circ}$
NorESM2–LM	(39)	$2.5^{\circ} \times 2^{\circ}$

2.1 Bias-correction Techniques

GCMs often produce biased results due to their coarse spatial resolutions. These biases require correction before utilizing climate projections in impact studies (40). This study employs the MeteoLab toolbox (https://meteo.unican.es/trac/MLToolbox (last access date: 2022/07/21)), encompassing both scaling-based correction and distribution-based correction methods. Scaling-based methods include the delta method, which adjusts future period simulations based on historical period differences, and the scaling method, which involves multiplying or adding scaling factors derived from the mean differences between observations and simulations in the reference period.

Quantile mapping methods (QM) are commonly used, as they can match all statistical moments of GCM outputs with observational data. These methods map the Cumulative Distribution Functions (CDFs) of GCM outputs from the historical period to those of observations. For future climate scenarios, the CDFs are computed based on GCM outputs from the historical period, considering GCM scenarios for the future. The corrected values for future periods are then extracted from the CDFs of the observations. Details of the eQM and aQM methods are elaborated in Amengual et al. (2012). The parametric quantile mapping method, gpQM, is based on a Gamma Generalized Pareto Distribution (GPD). Additionally, the isimip method, developed by Hempel et al. (2013) within the ISI-MIP project, preserves the change signal and can be applied to various variables, considering dependencies between some of them.

2.1 Comprehensive Rating Metrics (MR) and Taylor diagram

To determine the top-performing GCMs, a comprehensive assessment index named RM (as described by Jiang *et al.*, 2015) is employed. This index considers all statistical metrics in evaluation of GCM performance. The RM is characterized as:

$$MR = 1 - \frac{1}{mn}\sum_{i=1}^{n} rank_i$$

where m is the number of models, and n is the number of indices. A closer value of MR to 1 indicates a greater simulation skill.

GCMs are evaluated in capturing the historical precipitation (or temperature) spatial patterns using the Taylor diagram (26). This diagram serves as a means to compare GCMs with observed data, employing spatial metrics such as spatial CC, RMSD, and SD. Spatial CC quantifies the alignment of phase between two datasets, while spatial RMSD signifies the level of agreement in amplitude. A perfect simulation would entail an RMSD of 0, a spatial correlation near 1, and a spatial SD close to the observational data.

4. Results and Discussions

4.1 Evaluation of CMIP6-GCMs Performance and Generating Multi-Model Ensemble

To assess the performance of CMIP6 models, the GCM outputs are individually compared with reference data at each grid cell. Skill metrics, including CC, RMSE, bias, and SD, are then spatially averaged across the domain. Considering all skill metrics, a comprehensive rating index (MR) evaluates the models. Figure 2 (a) and (b) depict the statistical indices for precipitation and air temperature. In Figure 2 (a), it is evident that all CMIP6-GCMs exhibit a poor CC (< 0.4) in precipitation simulation. Most CMIP6 models show a positive spatially averaged bias in precipitation simulation, with FGOALS-g3 being the only exception, displaying a negative bias. MRI-ESM2-0 stands out among CMIP6-GCMs with the highest bias and RMSE of 21 and 34 mm, respectively. The standard deviation is computed relative to the reference data ($SD_{relative} = SD_{model} - SD_{ref}$), with MIROC6 offering the lowest $SD_{relative}$ values, around -1. In Figure 3(a), CMIP6-GCMs are ranked based on their ability to simulate the temporal variability of the Volga River basin's precipitation using skill metrics and the MR criterion. As stated in the research conducted by Ahmed et al., 2020, the best performance of Multi-Model Ensembles (MMEs) is attained when approximately half of the highest-ranked GCMs are incorporated. The six top-ranked GCMs for simulating monthly precipitation evolution over the Volga River basin are CEM2, CanESM5, MIROC-ES2L, CNRM-CM6-1, HadGEM3-GC31-LL, and IPSL-CM6A-LR.

Figure 4 (a) depicts the Taylor diagram illustrating CMIP6-GCM performance in simulating spatial variability of monthly precipitation. The time-averaged GCM

precipitation at each cell from 1950 to 2014 is compared with the reference data. Most models demonstrate spatial CC values ranging from 0.6 to 0.85, except for GISS-E2-1-G, which exhibits a CC of 0.3. The RMSD for the majority of models falls between 4-7 mm, while GISS-E2-1-G shows a higher RMSD of 10 mm. The $SD_{relative}$ for most models is below 8 mm, but CNRM-CM6-1, CNRM-ESM2-1, and GISS-E2-1-G have $SD_{relative}$ values between 8-10 mm. The Taylor diagram reveals that the six top-ranked GCMs for simulating temporal precipitation variability (Figure 3(a)) also capture spatial precipitation patterns over the Volga River basin well. A multi-model ensemble is generated by averaging these selected models to reduce individual model uncertainties.

Regarding temporal variability in air temperature, all CMIP6-GCMs exhibit high CC values exceeding 0.9 but display significant biases in air temperature (Figure 2(b)). Most CMIP6 models show a positive spatially averaged bias in simulating air temperature. However, BCC-CSM2-MR, FGOALS-g3, GISS-E2-1-G, HadGEM3-GC31-LL, and MIROC-ES2L demonstrate a negative bias in air temperature simulation, with HadGEM3-GC31-LL having the highest bias at approximately 3.8 °C. FGOALS-g3 shows the highest RMSE value, which is 5.6 °C. CanESM5, CNRM-ESM2-1, and CNRM-CM6-1 have $SD_{relative}$ values close to zero. According to Figure 3(b), the six top-ranked GCMs in simulating temporal variability of air temperature are CanESM5, CNRM-CM6-1, CNRM-ESM2-1, MIROC6, IPSL-CM6A-LR, and CEM2 (Figure 3(b)). The Taylor diagram in Figure 4(b) illustrates that most models exhibit spatial CCs within the range of 0.8 to 0.9, and the RMSD for most models is around 1°C. The $SD_{relative}$ for all models falls between 1.5 °C and 2.5 °C, with FGOALS-g3 showing a slightly higher $SD_{relative}$, nearing 3 °C. The Taylor diagram indicates that the top six GCMs for simulating temporal air temperature variability (Figure 4 (b)) demonstrate proficiency in reproducing spatial air temperature patterns over the Volga River basin. The multi-model ensemble for temperature is generated by averaging these selected models to reduce individual model uncertainties.

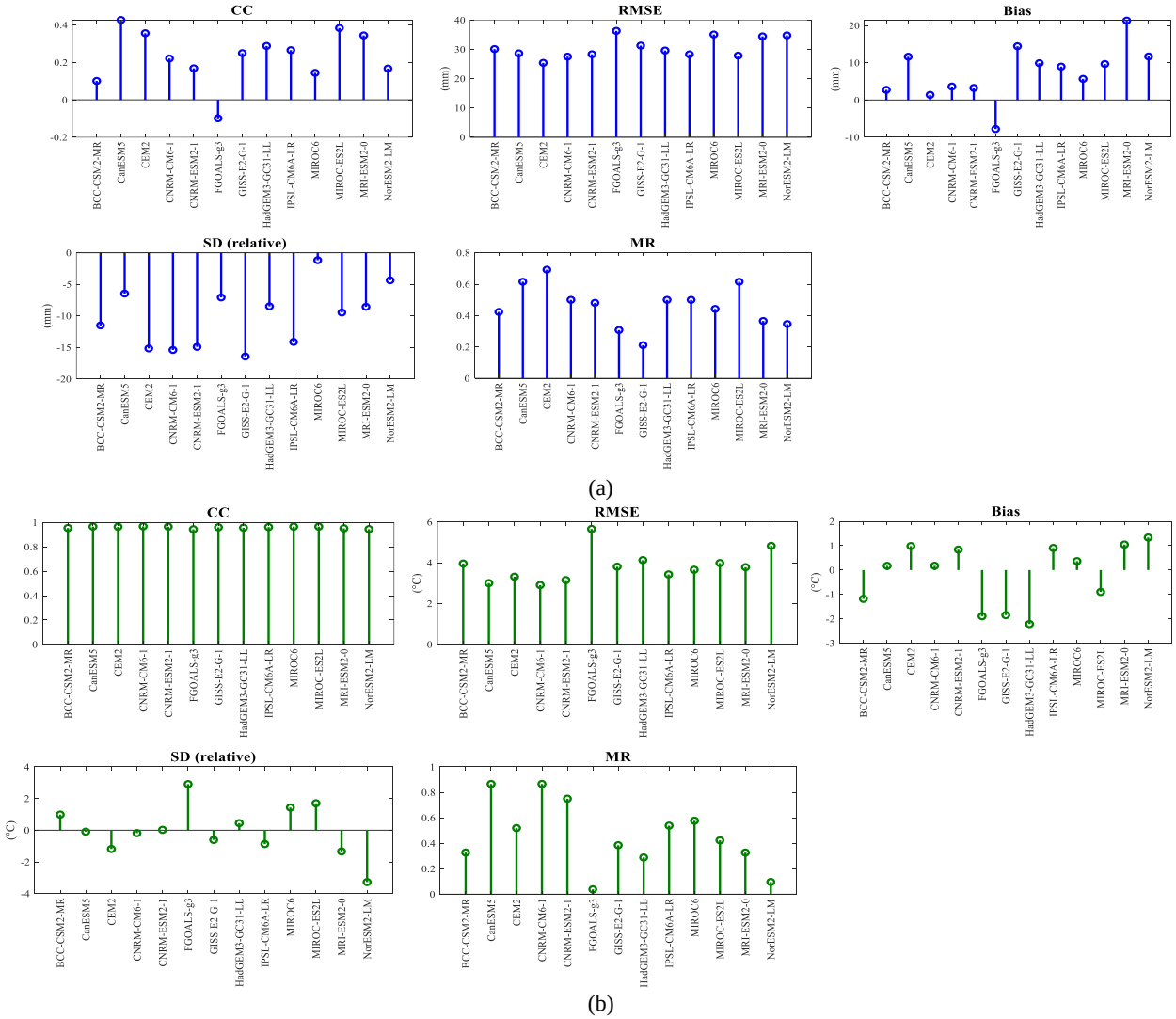

Fig. 2: Stem plot of spatially averaged statistical indices showing each CMIP6 models performance in simulating monthly precipitation (a) and air temperature (b) over the Volga River basin for the historical period (1950-2014

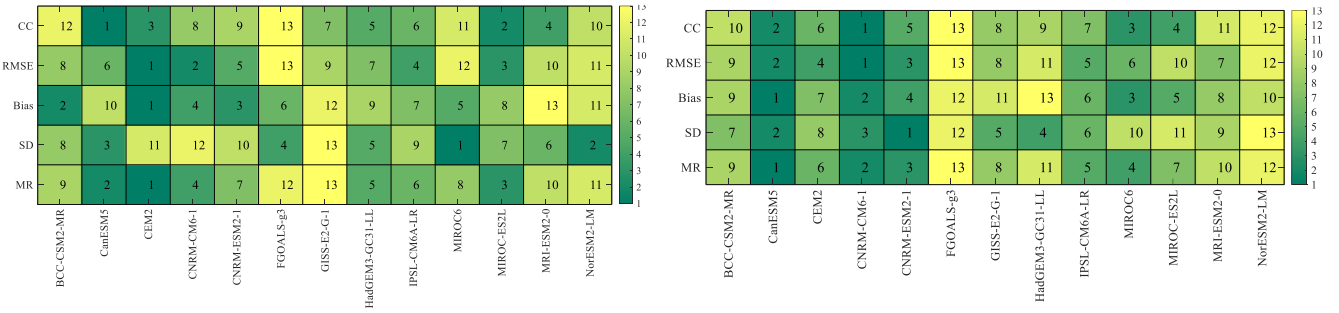

(a) (b)

Fig. 3: CMIP6 models rank in the simulation temporal variability of monthly precipitation (a) and air temperature (b) over the Volga River basin based on comprehensive rating metrics (MR)

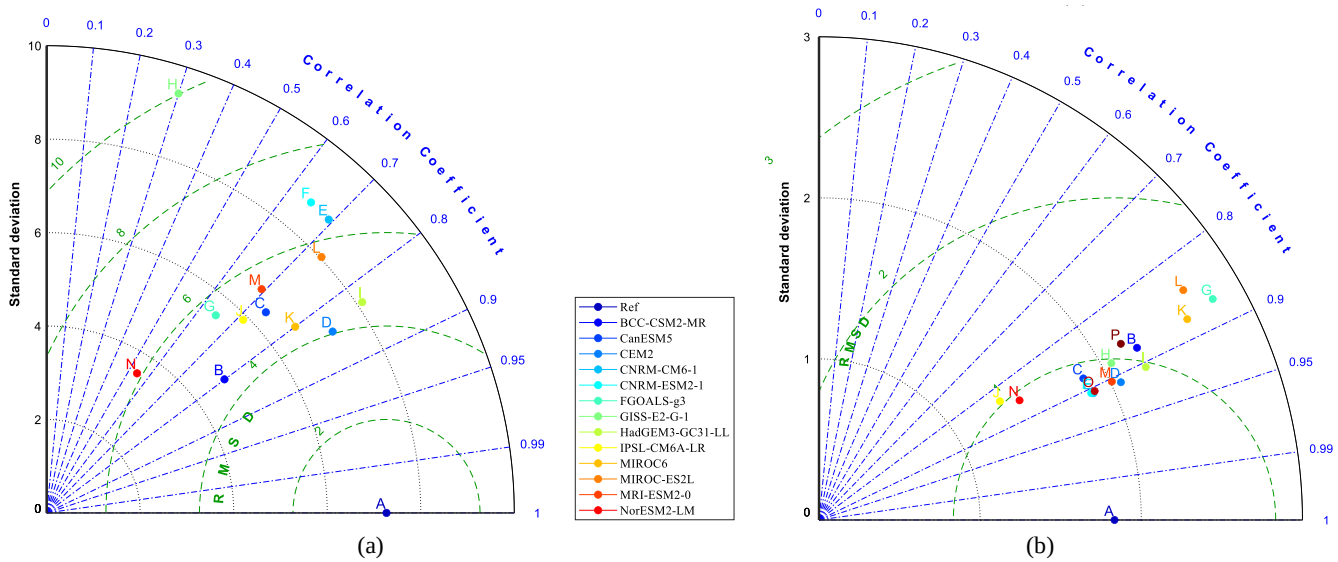

(a) (b)

Fig. 4: Taylor diagrams for monthly precipitation (a) and air temperature (b) over the Volga River basin comparing each of the CMIP6 models with the reference data for the historical period (1950–2014). The radial coordinate is the magnitude of the $SD_{relative}$ (indicated by solid black arcs). The concentric green semi-circles denote RMSD values. The angular coordinate shows the CC (indicated by dashed blue lines).

4.1 Evaluation Bias-correction Methods

Based on Figure 5 (a), it can be observed that the raw multi-model ensemble showed positive biases, leading to an overestimation of precipitation simulation. However, all the bias-correction methods proved to be effective in reducing these biases. The isimip and scaling methods performed well in terms of CC, RMSE, and MAE, although they exhibited lower performance in $SD_{relative}$. On the other hand, methods such as delta, eQM, aQM, and gpQM performed better in $SD_{relative}$ when compared to other indices. The mean_methods, which is an average of all the method outputs (aQM, delta, eQM, gpQM, isimip, and scaling), significantly improved bias and $SD_{relative}$ values, as demonstrated in Figure 5 (a). Additionally, these improvements extended to the spatial bias distribution over the Volga River basin, as depicted in Figure 5. Corrected precipitation via mean_methods also demonstrates improved spatial variability, as seen in Figure 4 (a).

According to Figure 5 (b), the raw multi-model ensemble displays positive biases, leading to an overestimated air temperature. Regarding temporal variability, all bias-correction methods, except for gpQM, significantly reduce RMSE, bias, MAE, and $SD_{relative}$. Spatially averaged CCs remain close to 1 across all methods. Thus, excluding gpQM, mean_methods is calculated by averaging the outputs of other methods (i.e., aQM, delta, eQM, scaling, and isimip). The spatial distribution of bias illustrates that employing mean_methods for bias-correction has decreased bias within the domain (Figure 7). Corrected air temperature via mean_methods also demonstrates improved spatial variability, as seen in Figure 4 (b).

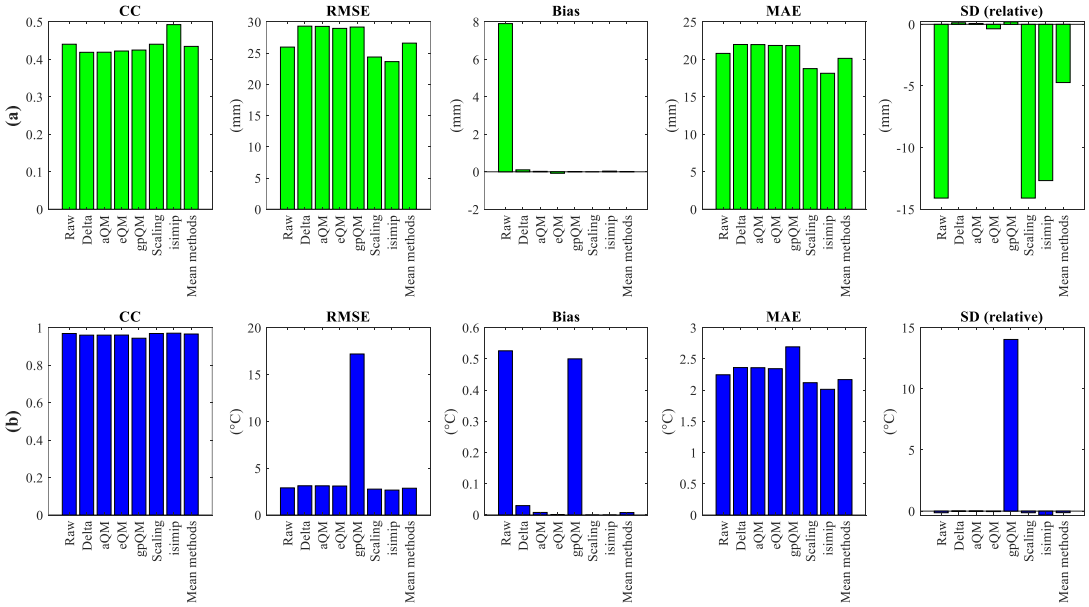

Fig. 5: Barchart of spatially averaged statistical indices showing each bias-correction methods performance in correcting monthly precipitation (a) and air temperature (b) over the Volga river basin for the historical period (1950-2014)

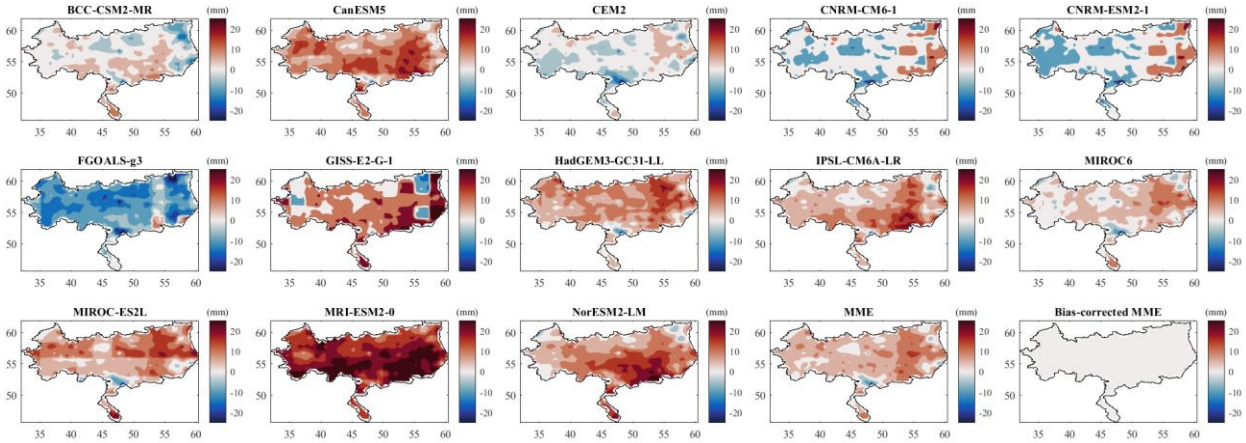

Fig. 6: Spatial maps of bias (mm) for simulating monthly precipitation over the study area (1950–2014)

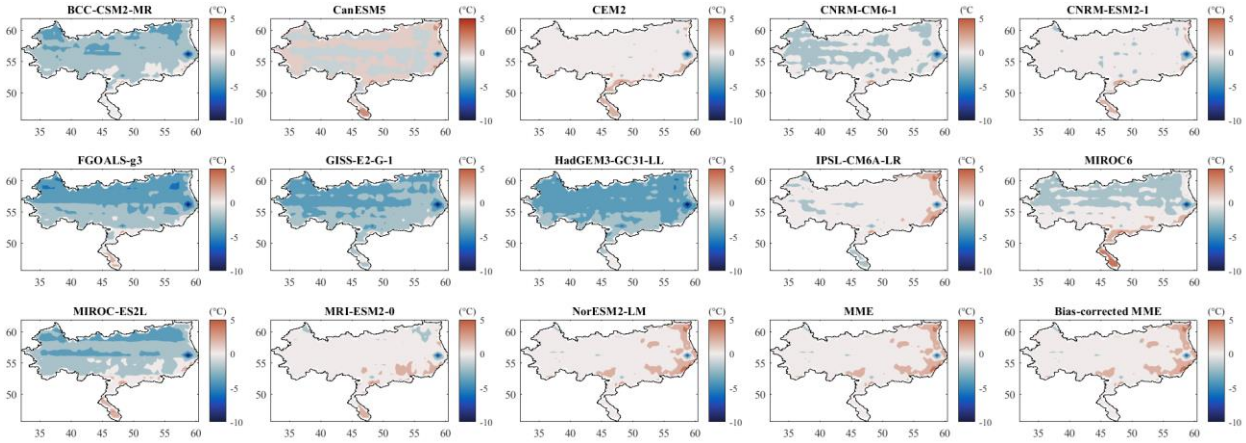

Fig. 7: Spatial maps of bias for simulating monthly air temperature over the study area (1950–2014)

4.1 Future Projections of Precipitation and Air Temperature

This study provides bias-corrected monthly precipitation and air temperature projections for the Volga River basin at a 0.5° resolution. These projections cover both historical (1950-2014) and future (2015-2100) time frames. The projected changes in annual mean precipitation and air temperature are presented over three temporal intervals: near future (2020-2046), mid future (2047-2073), and far future

(2074-2100), in comparison to the reference period (1988-2014). This result encompasses four different climate change scenarios: SSP1-2.6, SSP2-4.5, SSP3-7.0, and SSP5-8.5.

Figure 8 (a) depicts the time series of annual mean precipitation for the Volga River basin in the near, mid, and far future. This illustration reveals that by 2100, the annual mean precipitation in the Volga River basin is projected to rise to 476 mm under SSP1-2.6, 581 mm under SSP2-4.5, 610 mm under SSP3-7.0, and 610 mm under SSP5-8.5. The box plots in Figure 8 (b) show that between 2015 and 2100, the majority of precipitation changes (between quartiles 1 and 3) for the SSP1-2.6, SSP2-4.5, SSP3-7.0, and SSP5-8.5 scenarios are positive.

This result indicates that, in the future, under all climate change scenarios, precipitation over the Volga River basin will increase.

As shown in Figure 8 (b), in the near future, the increase in precipitation under SSP1-2.6 is greater than SSP5-8.5, and SSP5-8.5 exceeds scenarios SSP2-4.5 and SSP3-7.0. During 2020-2046, the spatially averaged annual mean precipitation is projected to increase by an average 8.1%, 5.2 %, 5.1 %, and 6.9 % under the SSP1-2.6, SSP2-4.5, SSP3-7.0, and SSP5-8.5 compared to the reference period respectively.

In the mid future, the increase in precipitation relative to the reference period is highest under SSP3-7.0, SSP2-4.5, SSP1-2.6, and SSP5-8.5, with average values of 13.1%, 13.8%, 14.4%, and 12.1%, respectively. During 2074-2100, the most substantial average increase in precipitation compared to the reference period is noted in SSP1-2.6, SSP2-4.5, SSP3-7.0, and SSP5-8.5, with values of 14%, 22%, 25%, and 29.3%, respectively.

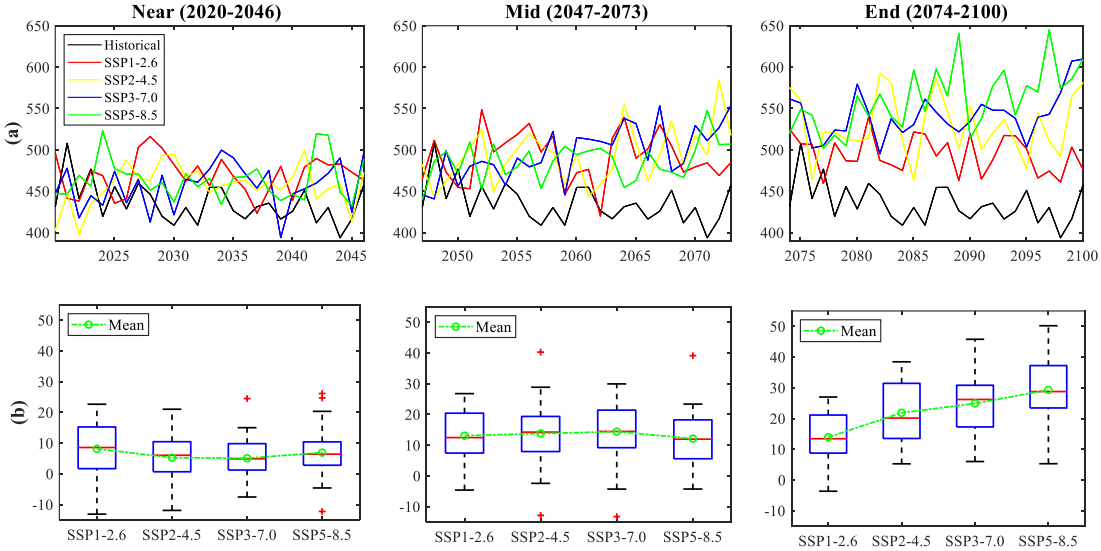

Fig. 8: (a) Time series and of spatially averaged annual mean precipitation over the Volga River basin, and (b) box plots of changes in annual mean precipitation over the CS in the near, mid, and far future relative to the historical data in the reference period under the SSP1-2.6, SSP2-4.5, SSP3-7.0, and SSP5-8.5 scenarios.

Figure 9 (a) displays a time series of spatially averaged annual mean air temperature over the Volga River basin for the near, mid, and far future under four different scenarios, along with historical data. In Figure 9 (a), it is evident that air temperature rises under all four scenarios over time. Specifically, by 2100, the annual mean air temperature for the Volga River basin is projected to increase to 5.9 °C under SSP1-2.6, 7.4 °C under SSP2-4.5, 9.3 °C under SSP3-7.0, and 10.9 °C under SSP5-8.5.

In the near future (2020-2046), SSP1-2.6 stands out with a slightly higher average annual mean air temperature compared to the other scenarios, while the remaining scenarios exhibit similar changes. As shown in Figure 9 (b), during this period, the spatially averaged annual mean air temperature is projected to increase by average 2 °C for SSP1-2.6 and approximately 1.7 °C for SSP2-4.5, SSP3-7.0, and SSP5-8.5 when compared to the reference period.

Moving into the mid future (2047-2073), there is a noticeable upward trend in air temperature changes, particularly evident in the first quartile, median, third quartile, and the mean across the scenarios from SSP1-2.6 to SSP5-8.5. During this period, the average increase in annual mean air temperature relative to the reference period is 2.8 °C for SSP1-2.6, 3.1 °C for SSP2-4.5, 3.4 °C for SSP3-7.0, and 3.9 °C for SSP5-8.5.

In the far future (2074-2100), the boxplot illustrates an even more pronounced increase in temperature, especially in all quartiles, and mean for the scenarios from SSP1-2.6 to SSP5-8.5. During this period, the average increase in annual mean air temperature relative to the reference period is 3 °C for SSP1-2.6, 4.2 °C for SSP2-4.5, 5.5 °C for SSP3-7.0, and 6.7 °C for SSP5-8.5.

To determine which climate scenario is closer to current conditions, the bias-corrected MMEs are compared with the

observational dataset for four scenarios. Since the GHCN dataset is available until the end of 2017, this comparison is conducted for 36 month period from the beginning of 2015 to the end of 2017 for precipitation and air temperature in the Volga River basin (Figure 10). The MR criterion is employed to assess the impact of three indices simultaneously: CC, MAE, and bias. According to Figure 10, SSP2–4.5 shows the highest MR value for precipitation, while both SSP1–2.6 and SSP2–4.5 have higher MR indices for temperature. Consequently, it can be inferred that SSP2–4.5 is the more likely scenario to represent the future climate of the Volga River basin.

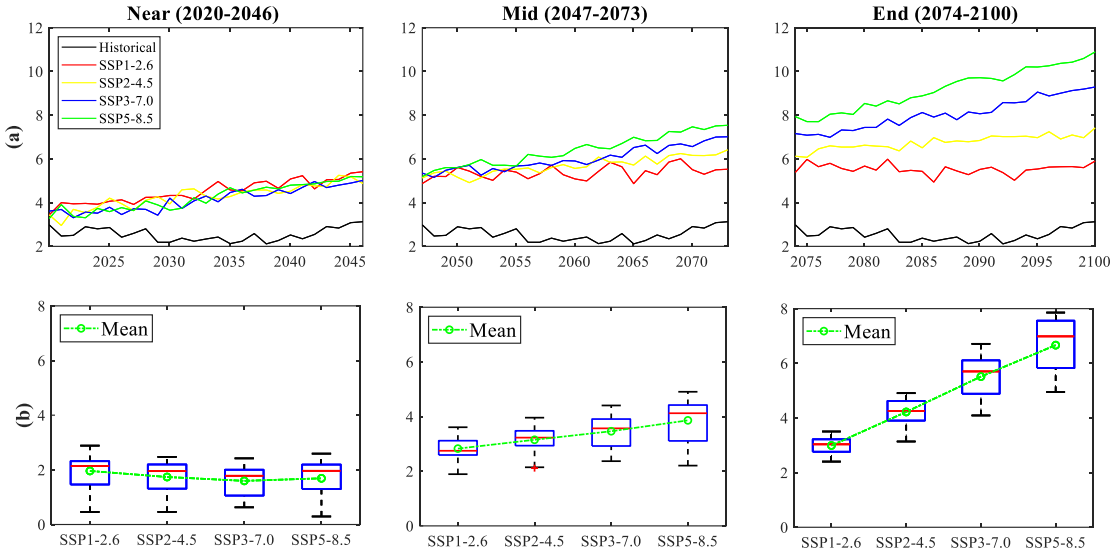

Fig. 9: (a) Time series of spatially averaged annual mean air temperature over the Volga River basin, and (b) box plots of changes in annual mean air temperature over the CS in the near, mid, and far future relative to the historical data in the reference period under the SSP1-2.6, SSP2-4.5, SSP3-7.0, and SSP5-8.5 scenarios.

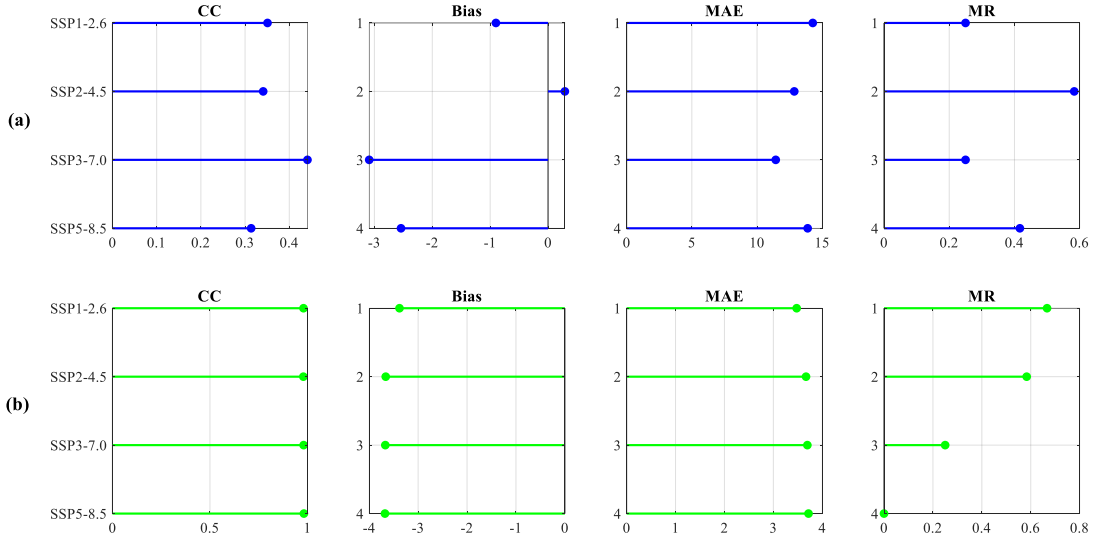

Fig. 6: Stem plot of statistical indices showing the agreement of each CMIP6 scenario with the precipitation (a) and air temperature (b) observational datasets over a 36-month period from 2015 to 2017.

5. Summary and Conclusion

This paper has presented future changes in precipitation and air temperature projections across the Volga River Basin using 13 CMIP6-GCM under SSP1–2.6, SSP2–4.5, SSP3–7.0, and SSP5–8.5 scenarios. This study offers valuable insights for future research on assessing the impact of climate change on the Volga River discharge, a major input of the Caspian Sea's water budget. These findings can inform decision-makers in developing mitigation and adaptation strategies.

Based on this research, the multi-model ensemble of the selected GCMs outperformed the individual models. Moreover, the statistical bias-correction techniques effectively reduced the uncertainties and corrected the biases in the CMIP6-GCMs. According to the evaluation metrics, corrected outputs were much more consistent with the observations compared to the raw outputs from GCMs. All bias-correction techniques (aQM, delta, eQM, gpQM,

isimip, and scaling) successfully reduced biases in the precipitation simulations. Regarding temperature, all methods employed in this paper, except for gpQM, effectively reduced bias. The isimip method effectively increases CC but underperforms in $SD_{relative}$.

The bias-corrected projections from the mean ensemble CMIP6-GCMs suggest the following range of changes (between quartiles 1 and 3) in precipitation and temperature changes in the Volga River basin:

The annual mean precipitation in the Volga River basin may increase between 0.7 to 15% during 2020-2046, depending on the scenario. Annual mean temperature changes in this period indicate warming in the Volga River basin, with projected air temperature increases ranging from 1°C to 2.2 °C, based on the scenario. The projected mean precipitation and temperature changes for the mid-term future (2047-2073) suggest that the Volga River basin may experience increased precipitation (5.6-21.4%) and higher temperatures (2.6°C to 4.4°C), depending on the scenario. Far future projections suggest that the Volga River basin could experience an annual mean precipitation increase of up to 37% and warming with annual mean temperature increases ranging from 2.8 °C to 7.6°C under different scenarios.

Increased air temperature leads to higher evaporation rates from the Volga River basin surface. If precipitation does not compensate for this increase, the Volga River discharge is likely to decrease in most scenarios.

While this study has addressed some uncertainties related to precipitation and air temperature projections in the Volga River basin, such as the choice of GCMs and bias correction methods, there are additional sources and methods that can further enhance the accuracy of the results. It is possible to conduct separate assessments and selection of GCMs for the different climate classes within the Volga River basin. Selecting a gridded observational dataset can be thoroughly accomplished by evaluating several station-based data and choosing the most suitable one for the Volga River basin. Future studies can incorporate these additional sources and methods to enhance the accuracy of precipitation and air temperature projections in the Volga River basin. Moreover, investigating future actual and potential evaporation over the Volga River basin is beneficial because it serves as an input for river-runoff models used to simulate future Volga River discharge.

References

1. Yue Y, Yan D, Yue Q, Ji G, Wang Z. Future changes in precipitation and temperature over the Yangtze River Basin in China based on CMIP6 GCMs. Atmos Res [Internet]. 2021;264(July):105828. Available from: https://doi.org/10.1016/j.atmosres.2021.105828
2. Mondal SK, Tao H, Huang J, Wang Y, Su B, Zhai J, et al. Projected changes in temperature, precipitation and potential evapotranspiration across Indus River Basin at 1.5–3.0 °C warming levels using CMIP6-GCMs. Sci Total Environ [Internet]. 2021;789:147867. Available from: https://doi.org/10.1016/j.scitotenv.2021.147867
3. Yazdandoost F, Moradian S, Izadi A, Aghakouchak A. Evaluation of CMIP6 precipitation simulations across different climatic zones: Uncertainty and model intercomparison. Atmos Res [Internet]. 2020;(September):105369. Available from: https://doi.org/10.1016/j.atmosres.2020.105369
4. Shrestha AB, Wagle N, Rajbhandari R. A review on the projected changes in climate over the Indus Basin. Indus River Basin. 2019;145–58.
5. Gusain A, Ghosh S, Karmakar S. Added value of CMIP6 over CMIP5 models in simulating Indian summer monsoon rainfall. Atmos Res [Internet]. 2020;232(September 2019):104680. Available from: https://doi.org/10.1016/j.atmosres.2019.104680
6. Ahmed K, Sachindra DA, Shahid S, Iqbal Z, Nawaz N, Khan N. Multi-model ensemble predictions of precipitation and temperature using machine learning algorithms. Atmos Res [Internet]. 2020;236:104806. Available from: https://www.sciencedirect.com/science/article/pii/S0169809519309858
7. Khan N, Shahid S, Ahmed K, Ismail T, Nawaz N, Son M. Performance assessment of general circulation model in simulating daily precipitation and temperature using multiple gridded datasets. Water (Switzerland). 2018;10(12).
8. Mishra V, Bhatia U, Tiwari AD. Bias-corrected climate projections for South Asia from Coupled Model Intercomparison Project-6. Sci Data [Internet]. 2020;7(1):1–13. Available from: http://dx.doi.org/10.1038/s41597-020-00681-1
9. Raju KS, Kumar DN. Review of approaches for selection and ensembling of GCMS. J Water Clim Chang. 2020;11(3):577–99.
10. Hoseini SM, Zolfaghari MR, Soltanpour M. Probabilistic estimates of future changes in evaporation from the Caspian Sea based on multimodel ensembles of CMIP6 projections. Int J Climatol. 2023;(March):5830–44.
11. Kattsov VM, Akentieva E, Aleksandrov E, Alekseev G, Anisimov O, Balonishnikova Z, et al. Report on climate risks in the Russian Federation. St Petersbg. 2017;106.
12. Rodionov SN. Global and regional climate interaction: the Caspian Sea experience. Global and regional climate interaction: the Caspian Sea experience. 1994.
13. Nesterenko YM, Solomatin N V., Nikiforov SE, Yu Nesterenko M, Kapustina OA. Climate changes analysis in the Volga Region and the Urals. IOP Conf Ser Earth Environ Sci. 2023;1154(1).
14. Georgiadi AG, Kashutina EA, Milyukova IP. Long Periods of Increased/Decreased Runoffs of Large Russian Rivers. IOP Conf Ser Earth Environ Sci. 2019;386(1).
15. Gelfan AN, Gusev EM, Kalugin AS, Krylenko IN, Motovilov YG, Nasonova ON, et al. Runoff of Russian Rivers under Current and Projected Climate Change: a Review 2. Climate Change Impact on the Water Regime of Russian Rivers in the XXI Century. Water Resour.

2022;49(3):351–65.

16. Kalugin A. Hydrological and Meteorological Variability in the Volga River Basin under Global Warming by 1.5 and 2 Degrees. Climate. 2022;10(7):1–23.
17. Beck HE, Zimmermann NE, McVicar TR, Vergopolan N, Berg A, Wood EF. Present and future köppen-geiger climate classification maps at 1-km resolution. Sci Data. 2018;5:1–12.
18. Eyring V, Bony S, Meehl GA, Senior CA, Stevens B, Stouffer RJ, et al. Overview of the Coupled Model Intercomparison Project Phase 6 (CMIP6) experimental design and organization. Geosci Model Dev. 2016;9(5):1937–58.
19. O'Neill BC, Tebaldi C, Van Vuuren DP, Eyring V, Friedlingstein P, Hurtt G, et al. The Scenario Model Intercomparison Project (ScenarioMIP) for CMIP6. Geosci Model Dev. 2016;9(9):3461–82.
20. Alexander LV, Zhang X, Peterson TC, Caesar J, Gleason B, Klein Tank AMG, et al. Global observed changes in daily climate extremes of temperature and precipitation. J Geophys Res Atmos. 2006;111(D5).
21. Willmott CJ, Matsuura K. Terrestrial Air Temperature and Precipitation: Monthly and Annual Time Series (1900 - 2017). http://climate.geog.udel.edu/~climate/html_pages/README.ghcn_ts2.html. 2018.
22. Muche ME, Sinnathamby S, Parmar R, Knightes CD, Johnston JM, Wolfe K, et al. Comparison and evaluation of gridded precipitation datasets in a Kansas agricultural watershed using SWAT. JAWRA J Am Water Resour Assoc. 2020;56(3):486–506.
23. Wang S, Li H, Zhang M, Duan L, Zhu X, Che Y. Assessing Gridded Precipitation and Air Temperature Products in the Ayakkum Lake, Central Asia. Sustain. 2022;14(17).
24. Liang-Liang L, Jian L, Ru-Cong Y. Evaluation of CMIP6 HighResMIP models in simulating precipitation over Central Asia. Adv Clim Chang Res. 2022;13(1):1–13.
25. Jiang Z, Li W, Xu J, Li L. Extreme precipitation indices over China in CMIP5 models. Part I: Model evaluation. J Clim. 2015;28(21):8603–19.
26. Taylor KE. Summarizing multiple aspects of model performance in a single diagram. J Geophys Res Atmos. 2001;106(D7).
27. Wu T, Lu Y, Fang Y, Xin X, Li L, Li W, et al. The Beijing Climate Center climate system model (BCC-CSM): The main progress from CMIP5 to CMIP6. Geosci Model Dev. 2019;12(4):1573–600.
28. Swart NC, Cole JNS, Kharin V V., Lazare M, Scinocca JF, Gillett NP, et al. The Canadian Earth System Model version 5 (CanESM5.0.3). Geosci Model Dev. 2019;12(11):4823–73.
29. Lauritzen PH, Nair RD, Herrington AR, Callaghan P, Goldhaber S, Dennis JM, et al. NCAR release of CAM-SE in CESM2. 0: A reformulation of the spectral element dynamical core in dry-mass vertical coordinates with comprehensive treatment of condensates and energy. J Adv Model Earth Syst. 2018;10(7):1537–70.
30. Voldoire A, Saint-Martin D, Sénési S, Decharme B, Alias A, Chevallier M, et al. Evaluation of CMIP6 deck experiments with CNRM-CM6-1. J Adv Model Earth Syst. 2019;11(7):2177–213.
31. Séférian R, Nabat P, Michou M, Saint-Martin D, Voldoire A, Colin J, et al. Evaluation of CNRM Earth System Model, CNRM-ESM2-1: Role of Earth system processes in present-day and future climate. J Adv Model Earth Syst. 2019;11(12):4182–227.
32. Li L, Yu Y, Tang Y, Lin P, Xie J, Song M, et al. The flexible global ocean-atmosphere-land system model grid-point version 3 (FGOALS-g3): description and evaluation. J Adv Model Earth Syst. 2020;12(9):e2019MS002012.
33. Kelley M, Schmidt GA, Nazarenko LS, Bauer SE, Ruedy R, Russell GL, et al. GISS-E2. 1: Configurations and climatology. J Adv Model Earth Syst. 2020;12(8):e2019MS002025.
34. Roberts MJ, Baker A, Blockley EW, Calvert D, Coward A, Hewitt HT, et al. Description of the resolution hierarchy of the global coupled HadGEM3-GC3. 1 model as used in CMIP6 HighResMIP experiments. Geosci Model Dev. 2019;12(12):4999–5028.
35. Boucher O, Servonnat J, Albright AL, Aumont O, Balkanski Y, Bastrikov V, et al. Presentation and evaluation of the IPSL-CM6A-LR climate model. J Adv Model Earth Syst. 2020;12(7):e2019MS002010.
36. Tatebe H, Ogura T, Nitta T, Komuro Y, Ogochi K, Takemura T, et al. Description and basic evaluation of simulated mean state, internal variability, and climate sensitivity in MIROC6. Geosci Model Dev. 2019;12(7):2727–65.
37. Hajima T, Watanabe M, Yamamoto A, Tatebe H, Noguchi MA, Abe M, et al. Development of the MIROC-ES2L Earth system model and the evaluation of biogeochemical processes and feedbacks. Geosci Model Dev. 2020;13(5):2197–244.
38. Yukimoto S, Kawai H, Koshiro T, Oshima N, Yoshida K, Urakawa S, et al. The Meteorological Research Institute Earth System Model version 2.0, MRI-ESM2. 0: Description and basic evaluation of the physical component. J Meteorol Soc Japan Ser II. 2019;97(5):931–65.
39. Seland Ø, Bentsen M, Seland Graff L, Olivié D, Toniazzo T, Gjermundsen A, et al. The Norwegian earth system model, noresm2–Evaluation of thecmip6 deck and historical simulations. Geosci Model Dev Discuss. 2020;1–68.
40. Gondim R, Silveira C, de Souza Filho F, Vasconcelos F, Cid D. Climate change impacts on water demand and availability using CMIP5 models in the Jaguaribe basin, semi-arid Brazil. Environ Earth Sci. 2018;77(15).
41. Amengual A, Homar V, Romero R, Alonso S, Ramis C. A statistical adjustment of regional climate model outputs to local scales: application to Platja de Palma, Spain. J Clim. 2012;25(3):939–57.
42. Hempel S, Frieler K, Warszawski L, Schewe J, Piontek F. A trend-preserving bias correction–the ISI-MIP approach. Earth Syst Dyn. 2013;4(2):219–36.

This article is an open-access article distributed under the terms and conditions of the Creative Commons Attribution (CC-BY) license.